

## Article

# Shungite Paste Electrodes: Basic Characterization and Initial Examples of Applicability in Electroanalysis

Michaela Bártová, Martin Bartoš, Ivan Švancara and Milan Sýs\*

Department of Analytical Chemistry, Faculty of Chemical Technology, University of Pardubice, Studentská 573, 532 10 Pardubice, Czech Republic; michaela.bartova@student.upce.cz (M.B.); martin.bartos@upce.cz (M.B.); ivan.svancara@upce.cz (I.Š.)

\* Correspondence: milan.sys@upce.cz; Tel.: +420-466-037-034

**Abstract:** This article introduces a new type of carbon paste electrode prepared from black raw shungite. In powdered form, this carbonaceous material was mixed with several nonpolar binders. The resulting shungite pastes were microscopically and electrochemically characterized. Mixtures of several pasting liquids with different contents of shungite powder were tested to select the optimal composition and compared with other types of carbon paste-based electrodes made of graphite and glassy carbon powder. In terms of physical and mechanical properties, shungite paste electrodes (ShPEs) formed a composite mass being like dense pastes from glassy carbon microspheres, having harder consistency than that of traditional graphitic carbon pastes. The respective electrochemical measurements with ShPEs were based on cyclic voltammetry of ferri-/ferro-cyanide redox pairs, allowing us to evaluate some typical parameters such as electrochemically active surface area, double-layer capacitance, potential range in the working media given, heterogeneous rate constant, charge-transfer coefficient, exchange current density, and open-circuit potential. The whole study with ShPEs was then completed with three different examples of possible electroanalytical applications, confirming that the carbon paste-like configuration with powdered shungite represents an environmentally friendly (green) and low-cost electrode material with good stability in mixed aqueous-organic mixtures, and hence with interesting prospects in electroanalysis of biologically active organic compounds. It seems that similar analytical parameters of the already established variants of carbon paste electrodes can also be expected for their shungite analogues.

**Keywords:** shungite; carbon pastes; microscopic study; electrochemical characterization; reaction kinetics; electroanalytical applications

**Citation:** Bártová, M.; Bartoš, M.; Švancara, I.; Sýs, M. Shungite Paste Electrodes: Basic Characterization and Initial Examples of Applicability in Electroanalysis. *Chemosensors* **2024**, *12*, 118. <https://doi.org/10.3390/chemosensors12070118>

Received: 31 May 2024  
Revised: 25 June 2024  
Accepted: 26 June 2024  
Published: 28 June 2024



**Copyright:** © 2024 by the authors. Licensee MDPI, Basel, Switzerland. This article is an open access article distributed under the terms and conditions of the Creative Commons Attribution (CC BY) license (<https://creativecommons.org/licenses/by/4.0/>).

## 1. Introduction

In general, a carbon paste electrode (CPE), invented by Adams in 1958 [1], is a particular type of the heterogeneous sensors widely applicable in electrochemistry and electroanalysis. CPEs are made up of carbon paste, representing a mixture of carbon/graphite powder with a binder/pasting liquid firmly packed into an electrode holder. In order to improve their physicochemical properties, commonly used graphitic powders can be replaced by alternate carbonaceous materials [2,3]. They are represented by some synthetic products, namely, powdered glassy carbon [4], acetylene black [5], milled carbon fibers [6], and carbon nanoparticles [7], including ball-shaped fullerenes [8], carbon nanohorns [9], both multi- and single-walled carbon nanotubes [10], and single-layer graphene sheets [11]. Yet another alternative is a very popular boron-doped diamond [12]. In addition to all these carbon-based materials, some special clays [13] or transition-metal carbides [14] are now also of interest.

At present, cheaper and more environmentally friendly natural carbonaceous materials like natural graphite [15] activated carbon [16], charcoal black [17], calcined petroleum coke [18], biochar [19,20], and so-called shungite are coming to the fore, especially

as the constituents of supercapacitors [21], photocatalysts [22], Li-ion battery anodes [23], environmentally friendly adsorbing agents [24], or in the configurations of electroanalytical devices [25].

Regarding the latter-mentioned shungite, which is a semi-trivial name for an amorphous metamorphic form of mineralized carbon, it is classified into five categories according to its carbon content [26]. With the highest content (up to 98% (*w/w*) carbon), we have the shungite type 1, also called noble or elite shungite, which is regarded as the most promising variant for electrochemical applications [25]. Solid electrodes made by grinding raw shungite stones were shown to be comparable to the commercial glassy carbon electrode [25]. However, all solid electrodes lack some of the advantages offered by composite materials, namely, extractive accumulation of the analyte into the pasting liquid and simple modification by mixing in a suitable modifier.

Quite surprisingly, among the myriad of various CPEs proposed during more than six decades of carbon pastes in electrochemistry and electroanalysis [2,3], there is no special study that has dealt with the configurations of the shungite paste type, except one report with more or less preliminary information [27]. Thus, there is still a space to fill up the existing gap and introduce for the first time such a shungite paste electrode (ShPE) in a study featuring respective microscopic and electrochemical characteristics, including a necessary comparison with the most widely used CPE and related glassy carbon paste electrode (GCPE) [28].

In this work, commercially available shungite powder with 50% (*w/w*) carbon has been selected and the basic physicochemical and electrochemical characterization of the corresponding ShPE carried out, including the optimization of the corresponding paste composition for use in both purely aqueous and mixed-solvent media. To demonstrate the electroanalytical usefulness of the new ShPE tested, three different applications have been examined, namely, (i) voltammetric detection of pesticide fenhexamid in 10% (*v/v*) methanolic medium, (ii) determination of vitamin B2 in acidic aqueous solutions for an ShPE modified with MnO<sub>2</sub> redox mediator, and, finally, (iii) potentiometric titration of surfactants with an ShPE containing 2-nitrophenyl octyl ether as the pasting liquid.

## 2. Materials and Methods

### 2.1. Reagents and Chemicals

Manganese (IV) oxide powder, ≥98.0% riboflavin (VB2), ≥98.0% fenhexamid (FNX), ≥98.5% potassium hexacyanoferrate (II) trihydrate, 98% sodium dodecyl sulfate (SDS), and cetylpyridinium chloride (CPC) were purchased from Merck KGaA (Darmstadt, Germany). Raw shungite powder (mesh: 1–20 μm) was obtained from Skywest Trading s.r.o. (Prague, Czech Republic), whereas carbon powder (≥5 μm; natural and chemically purified product from graphite mines in Český Krumlov, Czech Republic [15]) was purchased from Maziva Týn s.r.o. (Týn and Vltavou, Czech Republic), and glassy carbon powder (particle size: 2–10 μm [4]) from HTW Hochttemperatur-Werkstoffe GmbH (Thierhaupten, Germany). As the paste binders, silicone oil (SO) of viscosity ≥ 8000 cSt from Lučební závody (Kolín, Czech Republic), mineral oil (MO), paraffin wax (PW), tricresyl phosphate (TCP), vaseline (VA), and 99% 2-nitrophenyl octyl ether (NPOE), all coming from Merck, were selected. Organic solvents, such as ~96% ethanol, ≥99.9% methanol (MeOH), ≥99.9% acetonitrile, and ≥99.9% acetone originated from Honeywell (Seelze, Germany) and served to prepare the mixed working media.

Glacial acetic acid (85%), (*ortho*)phosphoric acid (H<sub>3</sub>PO<sub>4</sub>, 98.5%), boric acid (s), sodium hydroxide (98.5%), sodium dihydrogen phosphate dihydrate, sodium hydrogen carbonate, sodium carbonate, potassium chloride, and 35% hydrochloride acid were used for preparation of 0.1 mol L<sup>-1</sup> Britton Robinson buffers (BRB; pH 2–6), 0.1 mol L<sup>-1</sup> phosphate buffer (PB; pH 7), 0.1 mol L<sup>-1</sup> hydro-carbonate buffer (CB; pH 9), and 0.01 mol L<sup>-1</sup> HCl + 0.1 mol L<sup>-1</sup> KCl (pH 2), all being from Lach-Ner s.r.o. (Neratovice, Czech Republic).

Ultrapure water with resistivity of  $\geq 18.3 \text{ M}\Omega \text{ cm}$  was obtained from a Milli-Q® deionization unit from Merck Millipore (Burlington, MA, USA).

## 2.2. Apparatus

All voltammetric experiments were performed in a three-electrode configuration consisting of one type of a CPE as the working electrode, a reference Ag/AgCl reference electrode with a  $3 \text{ mol L}^{-1}$  KCl salt bridge from Metrohm (Herisau, Switzerland), and a platinum sheet from Elektrochemické detektory (Turnov, Czech Republic) completing the cell as the auxiliary electrode. All the specified electrodes were immersed into a voltammetric cell containing 10 mL of the working medium chosen and being connected to a potentiostat/galvanostat (type Autolab PGSTAT101) and controlled by Nova software (version 1.11.0), both again from Metrohm.

Potentiometric titrations were carried out in a titration flask containing 5 mL of  $0.01 \text{ mol L}^{-1}$  SDS solution agitated at 400 rpm and indicated by CPE/NPOE versus reference Ag/AgCl using a portable pH meter CPH 52 from Elteca (Turnov, Czech Republic). Each titration was performed by manual dosing of a titration reagent ( $0.01 \text{ mol L}^{-1}$  CPC), again with agitating at 400 rpm.

Scanning electron microscopy (SEM) utilizing the secondary-electron (SE) mode was the technique of choice for imaging the microstructures of the shungite powder and energy-dispersive X-ray spectroscopy (EDX) for semi-quantitative determination of impurities when using an SEM apparatus TESCAN VEGA3 SBU with an EDX probe Bruker X-Flash Detector 410-M from TESCAN s.r.o. (Brno, Czech Republic). In order to achieve a high resolution of individual particles, the shungite powder had to be gold-plated with a 2 nm layer before microscopic investigation.

## 2.3. Preparation of Shungite Paste Electrodes

The corresponding carbonaceous paste electrodes were prepared from the respective powder (graphite, glassy carbon, and shungite) and a liquid binder selected. The optimum ratio between these main constituents was 4:1 (*w/w*). These pastes were made by hand-mixing in a ceramic mortar for 10 min to ensure the homogeneous distribution of carbon particles throughout the mixture [29]. The resulting pastes were then packed into a cavity of Teflon® piston-driven electrode holders of our own design [30] with two holders of different surface diameter, 3 mm for voltammetric and 10 mm for potentiometric measurements.

The height of column of rather dense shungite paste in the holder's cavity had to be kept maximally 1 cm due to its difficult extrusion. Also, a freshly prepared shungite paste electrode had to be left unused at least for one day, which allowed it to achieve needful self-homogenization being necessary for stable electrochemical behavior, as generally recommended for all types of carbon pastes [2,29]. Finally, the surface of ShPEs or CPE was renewed manually by extruding a small portion of carbon paste and smoothing it with a filter paper.

## 2.4. Electrochemical Experiments

Voltammetric techniques, such as linear sweep voltammetry (LSV) and cyclic voltammetry (CV), were used for the electrochemical characterization of the carbonaceous paste electrodes. Studies of electrode kinetics were performed in  $1 \text{ mmol L}^{-1} \text{ K}_4[\text{Fe}(\text{CN})_6]$  in  $0.1 \text{ mol L}^{-1}$  PB (pH 7). Setting parameters of these techniques were as follows: potential step ( $E_{\text{step}}$ ) of 5.0 mV and scan rate ( $\nu$ ) ranging from 0.01 to  $1.0 \text{ V s}^{-1}$ . Unless stated otherwise, all the changes in experimental and instrumental conditions are listed in the legends of the corresponding figures.

### 3. Results and Discussion

#### 3.1. Microscopy of Shungite and Shungite Paste

In comparison with planarly structured graphite sheets (Figure 1A) or spatially arranged glassy carbon globules (Figure 1B) in the respective paste variants, the resulting shungite paste resembles an inhomogeneous conglomerate (Figure 1C). As can be seen in Figure 1D, powdered ground shungite is made up of sharp-edged particles whose size ranges from  $\geq 2 \mu\text{m}$  to  $10 \mu\text{m}$ , when even a few larger pieces may be found. Energy-dispersive X-ray (EDX) microanalysis (see Figure 2) shows that shungite powder contains approximately 50% carbon, 33% oxygen, 15% silicon, 2% aluminum, and 1% potassium, while the rest represents traces of magnesium, iron, and sulfur (all in *w/w*). The carbon is formed by the smallest particles, typically in micrometer range and only rarely reaching larger size. Such are represented mainly by quartz and some aluminosilicates of variable composition, although these minerals can also be found among fine particles. Impurities of sulfur and iron indicate the presence of pyrite in the raw shungite material.

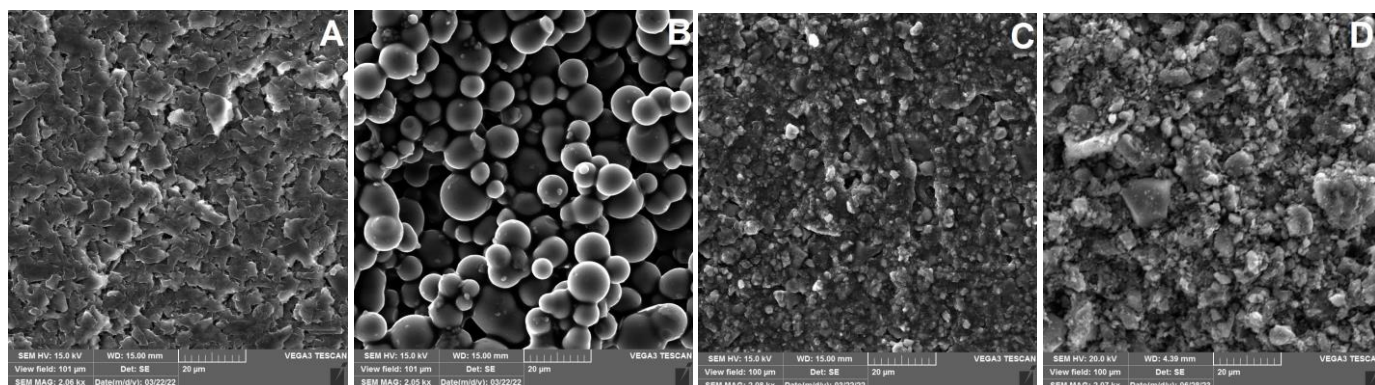


**Figure 1.** Detailed secondary electron images (SEM magnitude:  $\sim 2.05 \times 10^3$ ) of conventional CPE (A), GCPE (B), and ShPE (C), all with 20% (*w/w*) silicone oil content and commercially available shungite powder gold-plated with a 2 nm layer (D).

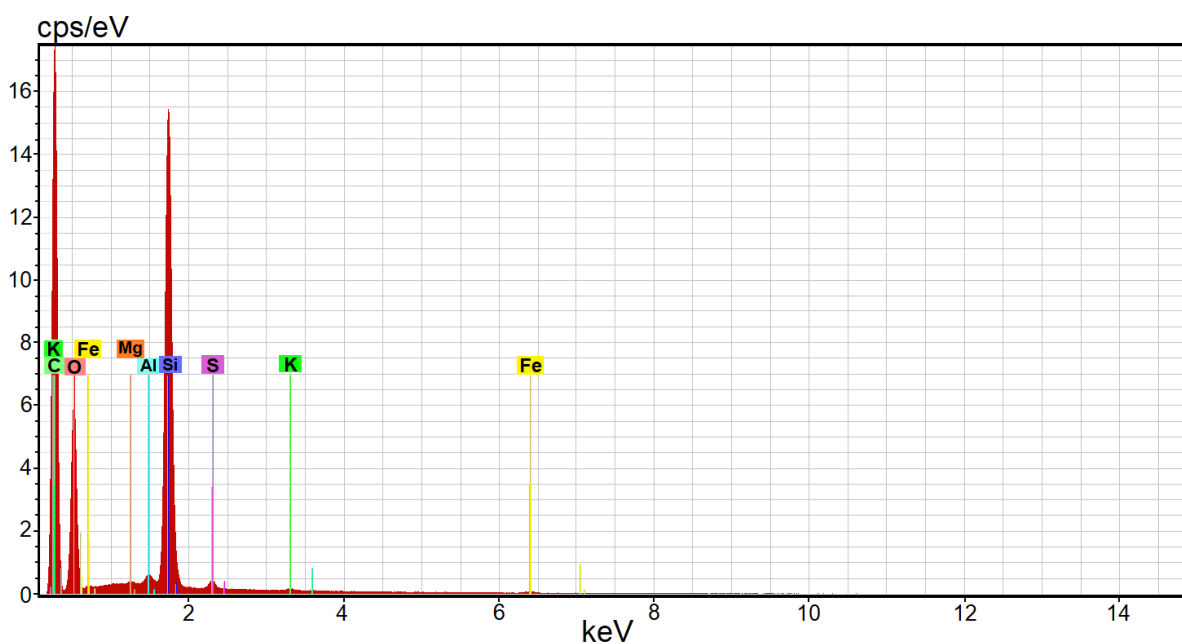


**Figure 2.** Energy-dispersive X-ray spectrum of the raw shungite powder purchased from Skywest Trading s.r.o. (Prague, Czech Republic).

### 3.2. Effect of the Carbon Paste Binder

At first, a general morphology of mixtures in Figure 1A,C corresponds quite well to our previous SEM studies with typical carbon pastes [4], having shown that solid particles of carbonaceous materials are almost totally covered by a very thin film of liquid binder. This is the case of both mixtures investigated herein made of irregular non-spherical shungite powder or from spherical glassy carbon particles [28] when the respective microstructures reveal very similar intimate coverage by molecules of the same density of silicone oil. Seven organic binders, namely, VA, MO, SO, PW, TCP, NPOE, and PP, were investigated as potentially suitable pasting liquids for the preparation of shungite paste electrode. Shungite pastes made of highly viscous binders, such as PW or SO (polydimethylsiloxane with molecular weight  $\geq 8000 \text{ g mol}^{-1}$ ) [29], and subsequently filled into a cavity of Teflon® piston-like electrode holder from University of Pardubice (Pardubice, Czech Republic) [30], look like solid composites. The other shungite pastes were very similar to their glassy carbon paste analogues, and regarding their consistency and physical properties, this means more plasticity. Nevertheless, they are still tighter than those prepared from common mineral or silicone oils [2,3].

### 3.3. Effect of Binder Content in Shungite Pastes on Their Physical Properties

Basically, graphite sheets [31] and spherical particles of glassy carbon [4,28] are not capable of absorbing a higher ratio of liquid binder than some nanomaterials, such as carbon nanotubes [10], graphene sheets [11], and carbon nanohorns [9]. The inability of the binder to penetrate onto the microstructure of non-porous carbonaceous materials makes the resulting pastes more viscous when the binder content exceeds 25–30% (*w/w*), because the individual particles are not in close contact, which is reflected in a principal increase in ohmic resistance [32]. The same phenomenon was also observed for shungite pastes, which could be expected because shungite powder represents more or less an aggregate of crumbs of amorphous carbonaceous rock (with irregularly shaped particles). Regardless of the type of binder used, shungite paste with content lower than 15% (*w/w*) forms a rather compact composite, which may inhibit surface renewal by otherwise effective mechanical wiping. By considering all the above facts, binder content between 15 and 20% (*w/w*) should be taken as optimum to obtain a paste mixture with suitable properties for electrochemical measurements.

### 3.4. Composition of the Working Medium

Numerous measurements using linear sweep voltammetry (LSV) performed in commonly used buffers of pHs ranging from 2 to 9 have shown that shungite paste is a stable heterogeneous material in all typical aqueous media. In addition, if such a paste is prepared from highly viscous silicone oil ( $\geq 8000 \text{ cSt}$ ) [33], it can then be characterized by good resistance towards the dissolution effect of polar organic solvents (MeOH, EtOH, MeCN, and acetone) and the respective mixtures withstand in media containing them up to 80% (*v/v*). In comparison with generally less stable graphitic pastes, the much better mechanical properties of silicone oil-based shungite pastes may significantly expand their application in the electrochemistry and electroanalysis of nonpolar organic substances. In addition, because of extractive/adsorptive accumulation of nonpolar electrochemically active substances onto ShPEs, there are further possibilities to adapt some ultrasensitive analytical methods for their use in extractive stripping voltammetry [2,3,33].

### 3.5. Electrochemical Characterization of Shungite Paste Electrode

Usually, important criteria obtainable during the electrochemical characterization of a new specific electrode material are sought with regard to its upcoming applications. Among them, one should evaluate potential ranges defined by the cathodic and anodic potential limits ( $E_{lim}^c$  and  $E_{lim}^a$ ), double-layer capacitance ( $C_{DL}$ ), kinetic parameters like heterogeneous rate constant ( $k^0$ ), charge-transfer coefficient ( $\alpha$ ), exchange current density

( $j_0$ ), and open circuit potential (OCP). All these characteristics were also investigated within this study with paste electrodes prepared from graphite, glassy carbon, or shungite powder, and the corresponding results and observations are presented separately in the following subsections.

### 3.5.1. Residual Current of Shungite Paste Electrode

The potential range of the new shungite paste has a major effect upon the scope of its electroanalytical utility [28]. In the case of shungite as such, its potential range can also be considered as a measure of electrochemical stability, allowing one to support the redox couples of battery chemistry, because even trace amounts of oxygen or hydrogen evolution are able to seriously deteriorate the cycle life of batteries [34].

Unlike for the CPEs and GCPEs tested, a gradual increase in the baseline response was observed for ShPEs, as can be seen in Figure S1 (belonging into Supplementary Materials). The ShPE displays almost comparably broad potential range as the other CPE variants mentioned above [28]. For a still-acceptable value of background currents of  $\sim 30 \mu\text{A cm}^{-2}$ , the widest potential range could be achieved in a neutral medium of  $0.1 \text{ mol L}^{-1}$  PB (pH 7), namely, from  $-1.4$  to  $+1.7$  V, whereas the shortest potential range ( $\geq 2.25$  V) was obtained in slightly alkaline solution of  $0.1 \text{ mol L}^{-1}$  CB (pH 9; from  $-1.0$  to  $+1.25$  V). Finally, the potential range ( $\geq 2.4$  V), defined by limiting values  $-0.95$  and  $+1.45$  V was determined for  $0.01 \text{ mol L}^{-1}$  HCl (pH 2).

### 3.5.2. Double-Layer Capacitance of Shungite Paste Electrode

As evident from Figure 3, the background (baseline) currents linearly increased with higher scan rates. The slope ( $k$ ) of the regression equation characterizing this relationship represents the double-layer capacitance ( $C_{\text{DL}}$ ) [35]. For aqueous solution of  $0.1 \text{ mol L}^{-1}$  KCl, a double-layer capacitance of  $\sim 10 \mu\text{F cm}^{-2}$  was found representing the  $C_{\text{DL}}$  value for a graphite-based paste electrode with non-activated carbon materials [36]. This was similar to  $C_{\text{DL}}$  values reported for different paste electrodes made of carbon black and silicone or mineral oil, all ranging from  $2.1$  to  $37.3 \mu\text{F cm}^{-2}$  [37].

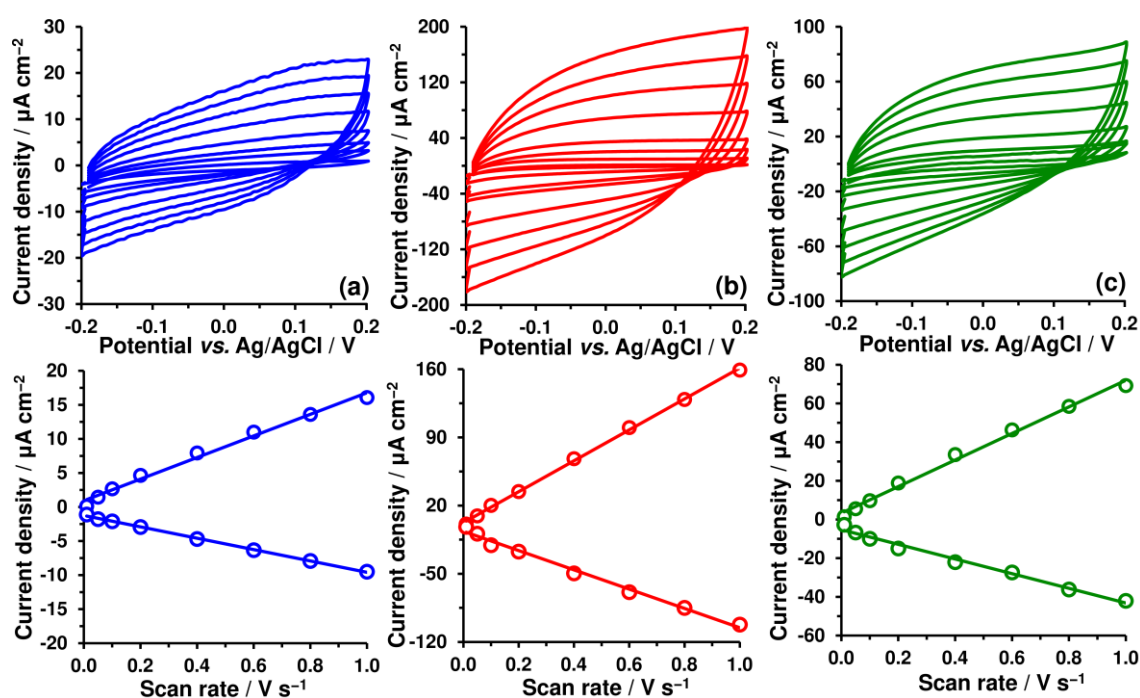


**Figure 3.** Double-layer-capacitance measurements obtained by cyclic voltammetry of  $0.1 \text{ mol L}^{-1}$  KCl recorded on conventional CPE (a), GCPE (b), and ShPE (c) at  $E_{\text{step}} = 5.0 \text{ mV}$  and  $\nu = 0.01, 0.05, 0.1, 0.2, 0.4, 0.6, 0.8,$  and  $1.0 \text{ V s}^{-1}$ . Associated figures represent plots of background-current response at  $0 \text{ V}$  vs. scan rate.

In contrast, the ShPE shows almost five times higher  $C_{DL}$  ( $\sim 50 \mu\text{F cm}^{-2}$ ), which is still at least two times lower than that for the GCPE ( $\sim 130 \mu\text{F cm}^{-2}$ ). Moreover, it was experimentally confirmed (Figure S2) that the CPE enriched by 10% ( $w/w$ ) non-covalently functionalized reduced graphene oxide (NFG) exhibited a double-layer capacitance of  $\sim 100 \mu\text{F cm}^{-2}$ . A similar value was achieved for the ShPE modified with only 5% NFG ( $w/w$ ), indicating some promise for applications as a structural supercapacitor [38].

From a practical point of view, paste mixtures from different carbonaceous powders can be considered to give rise to simple variants of composite materials, such as dispersion of carbon particles or graphene platelets from shungite rocks, in a highly viscous polymer [39], applicable in the development of supercapacitors.

### 3.5.3. Electrochemical Activity of Shungite Paste Electrode

At the solid-liquid interface, electrochemical activity is generally defined as a measure of the electron flow between a solid electrode and an electroactive substance in the working electrolyte solution and, therefore, it is considered to be one of the most important parameters for characterization of various electrode materials [40]. To compare the electrochemical activity of ShPEs with other paste electrodes, their performances were investigated by cyclic voltammetry in  $0.1 \text{ mol L}^{-1}$  PB (pH 7) containing  $1 \text{ mmol L}^{-1}$   $\text{K}_4[\text{Fe}(\text{CN})_6]$ , at a scan rate ranging from 50 to  $500 \text{ mV s}^{-1}$  (Figure 4).

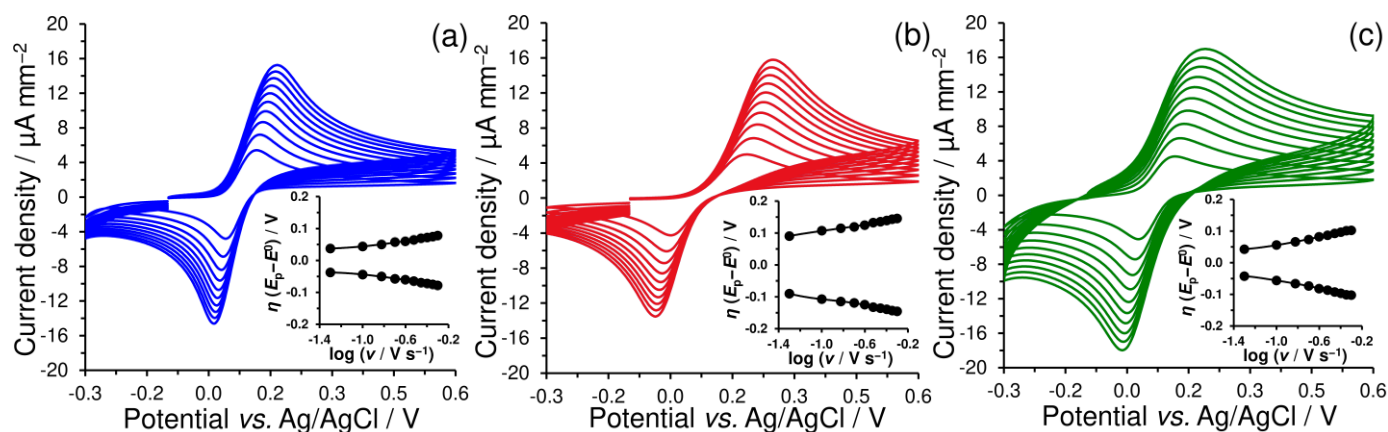


**Figure 4.** Cyclic voltammograms of  $1 \text{ mmol L}^{-1}$   $\text{K}_4[\text{Fe}(\text{CN})_6]$  in  $0.1 \text{ mol L}^{-1}$  PB (pH 7) recorded on conventional CPE (a), GCPE (b), and ShPE (c) at  $E_{\text{step}} = 5.0 \text{ mV}$  and  $\nu = 50, 100, 150, 200, 250, 300, 350, 400, 450,$  and  $500 \text{ mV s}^{-1}$ . Inserted figures represent the respective trumpet plots.

As can be assumed, the operational capabilities of paste electrodes fundamentally depend on the ratio between the powdered carbon moiety and pasting liquid, as well as upon the type and quality of both main paste constituents. For the constant content of silicone oil (20%  $w/w$ ), the comparable heterogeneous rate constants ( $k^0$ ) could be determined when using the Nicholson method [41] for the  $\text{Fe}^{2+}/\text{Fe}^{3+}$  redox couple in the CPEs and ShPEs, which is illustrated by the data in Table 1. Nearly the same  $k^0$  value of  $0.062 \text{ cm s}^{-1}$  was reported for optimal composition of the glassy carbon paste [28]. Since the shungite powder is made up of particles with diameter  $\geq 2 \mu\text{m}$  (comparable size of common graphite and glassy carbon in powdered form), almost identical values of electrochemically active surface area (ECSA) could be evaluated for the investigated trio of paste electrodes. Also, as shown by the values presented in Table 1, a content of 20% ( $w/w$ ) silicone oil in the paste mixture is not optimal in the case of the glassy carbon paste, reflected in twice-higher peak separation ( $\Delta E_p$ ) and a slightly higher ratio of the peak currents ( $I_p^c/I_p^a$ ).

**Table 1.** Overview of calculated electrochemical parameters.

Sensor	$R/\Omega \text{ cm}$	$ECSA/\text{cm}^2$	$\Delta E_p/\text{mV}$	$I_p^c/I_p^a$	$k^0/\text{cm s}^{-1}$	$\alpha_a$	$OCP/\text{V}$	$j_0/\text{A cm}^{-2}$
CPE	4.6	0.066	88.0	1.051	0.0084	0.52	-0.133	$7.9 \times 10^{-8}$
GCPE	9.2	0.061	214.6	1.105	0.0011	0.52	-0.141	$1.6 \times 10^{-7}$
ShPE	80.0	0.079	112.2	0.937	0.0063	0.50	-0.085	$1.3 \times 10^{-7}$

Notes: Data (excluding the first four) were obtained from cyclic voltammetry of 0 and 1 mmol L<sup>-1</sup> K<sub>4</sub>[Fe(CN)<sub>6</sub>] for carbon paste electrodes with 20% (w/w) silicone oil content in 0.1 mol L<sup>-1</sup> PB (pH 7) at scan rates ranging from 50 to 500 mV s<sup>-1</sup>.

Furthermore, Figure 5 depicts the Tafel plots for the [Fe(CN)<sub>6</sub>]<sup>4-</sup>/[Fe(CN)<sub>6</sub>]<sup>3-</sup> redox couple obtained for all the types of paste electrodes. The linear relationships between overpotential ( $\eta$ ) and logarithm of current density ( $j$ ), the so-called Tafel behavior, were found by extrapolation ( $R^2 > 0.9957$ ) and yielding the values of the exchange current densities ( $j_0$ ) and anodic barrier symmetry factor ( $\beta_a$ ), which could be replaced by the anodic charge-transfer coefficients ( $\alpha_a$ ) for the single-step reaction Fe<sup>2+</sup> to Fe<sup>3+</sup> investigated [42]. As the exchange current density indicates the spontaneous reaction rate at equilibrium potential, it can be deduced that shungite paste and glassy carbon paste ( $\sim 1.5 \times 10^{-7}$  A cm<sup>-2</sup>) are superior in this respect to traditional graphite pastes, as evident from values in Table 1. The calculated  $\alpha_a$  values close to a theoretical value of 0.5 then suggest that anodic oxidation is not favored over cathodic reduction and vice versa, which is also illustrated by symmetrical curves in the trumpet plots in Figure 4.

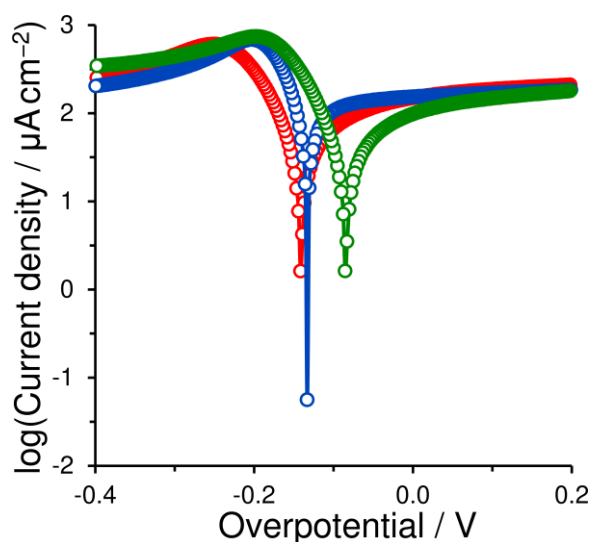


**Figure 5.** Tafel plots for the CPE (blue), GCPE (red), and ShPE (green curve) immersed in 0.1 mol L<sup>-1</sup> PB (pH 7) in the presence of 1 mmol L<sup>-1</sup> K<sub>4</sub>[Fe(CN)<sub>6</sub>] at a scan rate of 100 mV s<sup>-1</sup>.

Since open-circuit potential (OCP) represents the electrode potential at which no current flows between the working electrode and the reference, the immersed working electrode adopts the OCP, which defines its ability to be either oxidized or reduced [43]. As documented in Table 1, the OCP of paste electrodes vs. SCE increases in the order GCPE < CPE < ShPE, revealing a slightly higher thermodynamic stability of ShPEs, hence their lesser readiness to be oxidized. This fact is then confirmed by the gradual increase in the background currents during the LSV experiments, as seen in Figure S1.

### 3.6. Three Examples of Electroanalytical Applicability of Shungite Paste Electrodes

This section offers a first insight into electroanalytical utility of ShPEs, when three examples are selected to demonstrate, mainly, some specific features of the shungite-based paste revealed during our introductory characterization described in the previous sections.

### 3.6.1. Voltammetric Analysis of Fungicide Fenhexamid

In electroanalysis of pesticides, CPEs and related configurations have always been quite a frequent choice, and respective methods comprise a wide spectrum of analytes with respect to their chemical composition or use in agriculture [2,3]. To examine the electroanalytical performance of ShPEs in aqueous-organic mixtures, a fungicide fenhexamid (FNX) used as the active ingredient of Teldor® SC from Bayer (Leverkusen, Germany) was deliberately selected due to its low solubility in purely aqueous working media. Thus, the electrode tested should exhibit a certain degree of stability in the presence of organic solvents. As can be seen in Figure 6, in a buffer with 10% (*v/v*) MeOH, it gives rise to a well-developed anodic peak, slightly broader due to a more deformed baseline, but, in overall, comparable to an analogical response at the parent GCPE [44]. Then, after investigating electroanalytical performance of both paste electrodes under comparison, practically the same results can be achieved. This is documented by the corresponding linear ranges (from 2 to  $\geq 100 \mu\text{mol L}^{-1}$  FNX for GCPE and from 2.4 to  $\geq 100 \mu\text{mol L}^{-1}$  FNX for ShPE), and the slope values  $2.365 \mu\text{A cm}^{-2} \mu\text{mol}^{-1} \text{L}$  with  $R^2 = 0.9957$  for GCPE and  $2.2511 \mu\text{A cm}^{-2} \mu\text{mol}^{-1} \text{L}$  with  $R^2 = 0.9970$  for ShPEs, both paste mixtures containing the same amount of 20% (*w/w*) silicone oil. Initial values of linear ranges represent limits of quantification (LOQ), which were calculated according to the already known equation  $\text{LOQ} = 10s/k$ , where  $s$  is the standard deviation of repetitive measurements of  $10 \mu\text{mol L}^{-1}$  FNX ( $N = 5$ ) and  $k$  is the slope of the corresponding calibration curves. Otherwise, these essays have confirmed that ShPEs can serve in the same way as GCPEs, being known for their stability in mixed supporting media, in which traditional CPEs composited from common graphite are generally vulnerable.

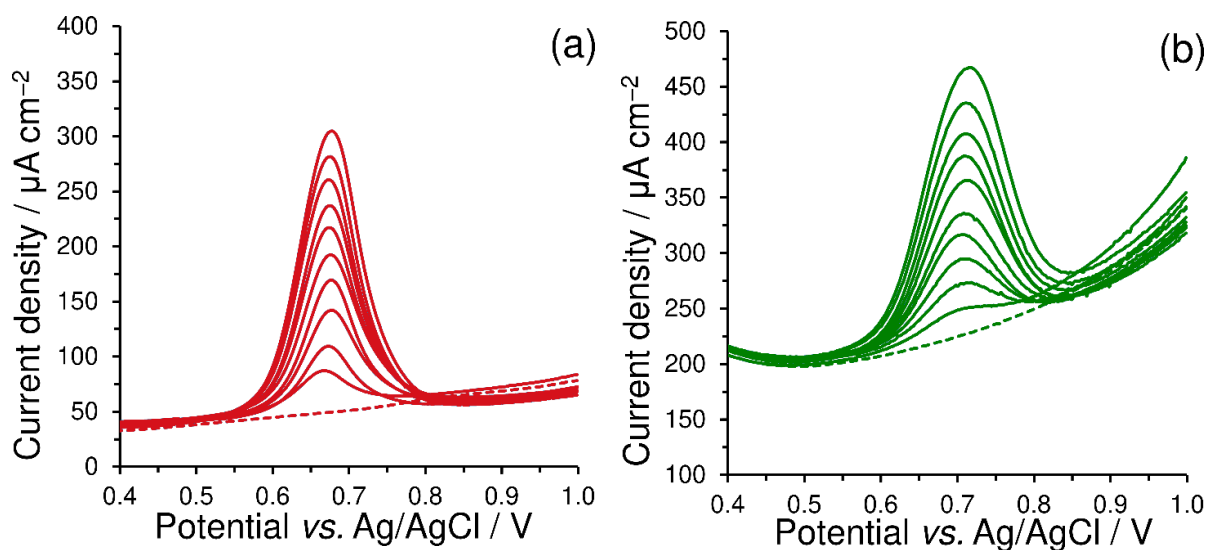


**Figure 6.** Voltammograms of 0 (dotted line), 10, 20, 30, 40, 50, 60, 70, 80, 90, and 100  $\mu\text{mol L}^{-1}$  FNX (solid lines) obtained for GCPE (a) and ShPE (b) in 0.1 mol  $\text{L}^{-1}$  BRB containing 10% (*v/v*) MeOH (pH 4) when using SWV at  $E_{\text{step}} = 5.0 \text{ mV}$ ,  $E_{\text{ampl}} = 30 \text{ mV}$ , and  $f = 40 \text{ Hz}$ .

### 3.6.2. Voltammetric Analysis of Vitamin B2

Also, vitamins often belong among determined analytes for carbon paste-based electrodes in numerous configurations comprising both bare (unmodified) and modified variants. The samples of interest were usually various food supplements or pharmaceutical formulations [45], a typical example being a manganese dioxide-modified CPE for voltammetric determination of riboflavin (VB2) [46]. The electrode of this type was also chosen for this second example tested in two variants as CPE/ $\text{MnO}_2$  and its shungite analogue (ShPE/ $\text{MnO}_2$ ) when using differential pulse voltammetry (DPV), as shown in Figure 7.

Linear dependencies of the current density on the logarithm of the VB2 concentration (0.1–10  $\mu\text{mol L}^{-1}$ ) can be obtained for both variants, which can be described by equations and characterized by coefficient of determinations, namely,  $j = 35.424\log c + 16.078$  with  $R^2 = 0.9963$  for CPE/MnO<sub>2</sub> and  $j = 10.532\log c + 3.114$  with  $R^2 = 0.9966$  for ShPE/MnO<sub>2</sub>.

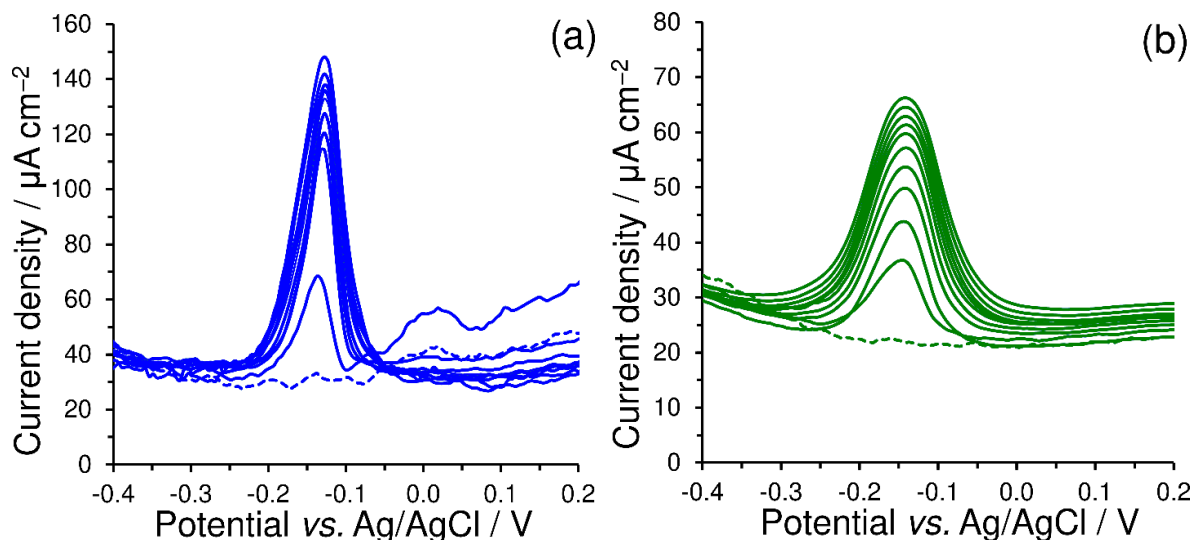


**Figure 7.** Voltammograms of 0 (dotted line), 1, 2, 3, 4, 5, 6, 7, 8, 9, and 10  $\mu\text{mol L}^{-1}$  VB2 (solid lines) obtained for CPE/MnO<sub>2</sub> (a); voltammograms of 0 (dotted line), 2, 4, 6, 8, 10, 12, 14, 16, 18, and 20  $\mu\text{mol L}^{-1}$  VB2 (solid lines) obtained for ShPE/MnO<sub>2</sub> (b). Supporting electrolyte: 0.1 mol L<sup>-1</sup> BRB (pH 2); DPV mode,  $E_{\text{step}} = 5$  mV,  $E_{\text{ampl}} = 25$  V, and  $\nu = 50$  mV s<sup>-1</sup>.

Despite a markedly lower sensitivity for ShPE/MnO<sub>2</sub>, it was still possible to achieve a very low LOQ of 91.3 nmol L<sup>-1</sup> VB2, which suggests that ShPEs can also be purposely modified like other CPEs. Furthermore, theoretical values of detection limits (LOD) were calculated to be 6.9 nmol L<sup>-1</sup> VB2 for CPE/MnO<sub>2</sub> and 27.4 nmol L<sup>-1</sup> VB2 for ShPE/MnO<sub>2</sub> according to the already known equation  $\text{LOD} = 3.3s/k$ , where  $s$  is the standard deviation of repetitive measurements of 1  $\mu\text{mol L}^{-1}$  VB2 for CPE/MnO<sub>2</sub> or 2  $\mu\text{mol L}^{-1}$  VB2 for ShPE/MnO<sub>2</sub> ( $N = 5$ ) and  $k$  is the slope of the corresponding calibration curves.

### 3.6.3. Potentiometric Indication in Titrations of the Surfactants

Besides conventional acid-base titrations [47], a solid shungite electrode covered with ion-selective membrane has already been introduced as an interesting alternate indicator electrode for potentiometric determination of the total content of anionic and cationic surfactants [25]. Figure 8 illustrates the possibility of using a special carbonaceous paste with 2-nitrophenyl octyl ether (NPOE) as a pasting liquid, allowing one to extract some ion-pairs which can then be adapted for potentiometric titration of surfactants without need to use an ion-selective membrane. That such an indicator as a CPE is functioning properly can be documented on a set of titration curves whose steep potential jumps reflect the content of 2-nitrophenyl octyl ether in the paste, as well as the type and amount of carbonaceous material used. Comparable maximum values of potential jump were obtained for paste electrodes containing 40% NPOE in CPEs, 30% NPOE in GCPEs, and 20% NPOE in ShPEs. When evaluating the depicted curves from an economic point of view, it seems more advantageous to choose rather cheap shungite powder, because its use also significantly reduces the required amount of pasting liquid in the paste mixture.

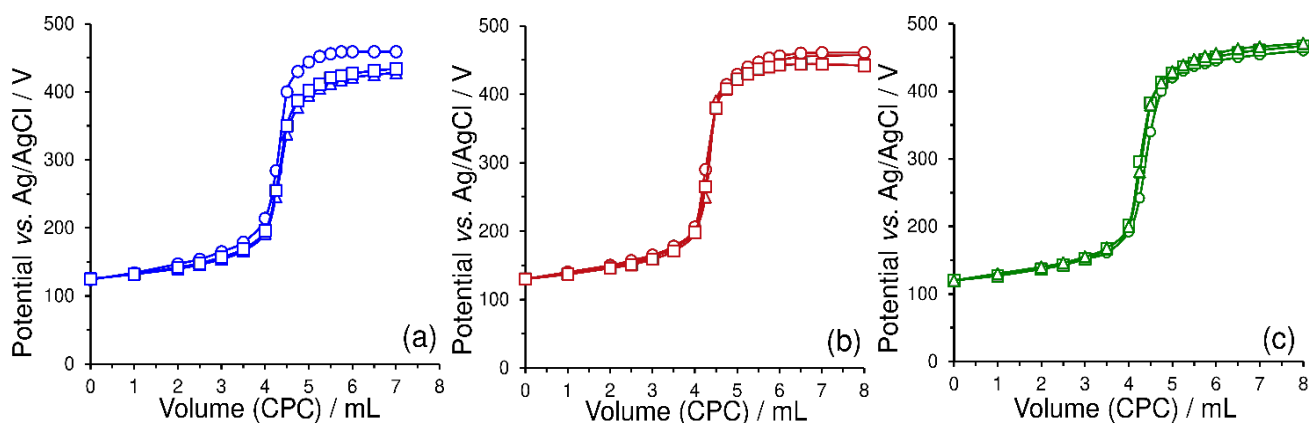


**Figure 8.** Typical potentiometric curves for three repetitive titrations of 5 mL  $0.01 \text{ mol L}^{-1}$  SDS solution titrated against  $0.01 \text{ mol L}^{-1}$  CPC solution when using CPE/40%NPOE (a), GCPE/30%NPOE (b), and ShPE/20%NPOE (c), all in *w/w*.

#### 4. Conclusions

In this article, shungite in a fine powdered form is used as a carbonaceous moiety in the paste-like configuration, giving rise to a special type of CPE that can be classified as a shungite paste electrode (ShPE). As found in our initial physicochemical and electrochemical characterization, the shungite paste exhibits more or less similar microscopic structure to traditional carbon pastes made of graphitic carbon. In contrast to them, shungite paste is denser and looks like a composite, which is apparently given by rather rough particles with highly irregular shapes (like miniature cornflakes) allowing them to be coated more tightly with the pasting liquid.

Regarding electrochemical characterization and some studies dealing with reaction kinetics, the shungite paste behaves similarly to traditional carbon pastes from powdered graphites, but in overall it is closer to a special paste-like mixture made of glassy carbon powder. This is because of the above-mentioned harder consistency, due to which the shungite paste exhibits enhanced stability in the presence of organic solvents in the supporting electrolyte, which can be advantageous in electroanalytical measurements with numerous organic and biological compounds. On the other hand, the very tough consistency of shungite paste is also behind a more difficult manipulation with its filling into the cavity of the electrode holder. Finally, this feature is also a probable reason for somewhat higher background currents in voltammetric measurements.

It should be emphasized also here that this study has for the first time proved the functionality of powdered shungite in the configuration of CPEs. For this purpose, one can see a certain likeness with natural graphite which was unearthed in local graphite mines in South Bohemia [15] and has repeatedly been shown to be fully comparable to graphites traditionally used for spectroscopy. Also, as powders, both shungite and natural graphite share one indisputable advantage, namely, that they are far less expensive than synthetic carbonaceous products, including the above-mentioned spectroscopic graphites or often preferable new forms of carbon nanomaterials.

In a wider perspective, shungite pastes seem to be applicable in specific electroanalytical devices, for instance, as miniature sensors and electrode cells for portable electrochemical analyzers which could find broad applications in various fields of industry. In addition, one can predict that heterogenous materials composed of shungite powder have some promise for fabrication of supercapacitors or anodes applicable in lithium-ion secondary batteries.

**Supplementary Materials:** The following supporting information can be downloaded at: <https://www.mdpi.com/article/10.3390/chemosensors12070118/s1>, Figure S1: Linear sweep voltammograms of  $0.1 \text{ mol L}^{-1}$  PB (pH 7) recorded on CPEs (blue), GCPEs (red), and ShPEs (green curve) at a scan rate of  $\nu = 50 \text{ mV s}^{-1}$ ; Figure S2: Double-layer-capacitance measurements obtained by cyclic

voltammetry of 0.1 mol L<sup>-1</sup> KCl recorded on CPE modified with 10% (*w/w*) reduced graphene oxide at  $E_{\text{step}} = 5.0$  mV and  $\nu = 0.01, 0.05, 0.1, 0.2, 0.4, 0.6, 0.8,$  and  $1.0$  V s<sup>-1</sup> (left). The associated figure plots the dependence of background-current response at 0 V on scan rate (right); Figure S3: The corresponding calibration curves of VB2 obtained at CPE/MnO<sub>2</sub> (blue) ShPE/MnO<sub>2</sub> (green) in 0.1 mol L<sup>-1</sup> BRB containing 10% (*v/v*) MeOH (pH 4) when using SWV at  $E_{\text{step}} = 5.0$  mV,  $E_{\text{ampl}} = 30$  mV, and  $f = 40$  Hz.

**Author Contributions:** formal analysis, M.B. (Michaela Bártová); formal analysis, M.B. (Martin Bartoš); methodology, conceptualization, and writing—review and editing, I.Š. (Ivan Švancara); formal analysis, conceptualization, methodology, writing—original draft and review, visualization, and supervision, M.S. (Milan Sýs). All authors have read and agreed to the published version of the manuscript.

**Funding:** This research received no external funding.

**Institutional Review Board Statement:** Not applicable.

**Informed Consent Statement:** Not applicable.

**Data Availability Statement:** All the relevant data are only provided in the present paper.

**Acknowledgments:** Financial support from the Faculty of Chemical Technology, University of Pardubice (project No. SGS\_2024\_004) is gratefully acknowledged.

**Conflicts of Interest:** The authors declare no conflicts of interest.

## References

1. Adams, R.N. Carbon paste electrodes. *Anal. Chem.* **1958**, *30*, 1576. <https://doi.org/10.1021/ac60141a600>.
2. Švancara, I.; Kalcher, K.; Walcarius, A.; Vytřas, K. *Electroanalysis with Carbon Paste Electrodes*, 1st ed.; CRC Press: New York, NY, USA, 2012.
3. Švancara, I.; Walcarius, A.; Kalcher, K.; Vytřas, K. Carbon paste electrodes in the new millennium. *Cent. Eur. J. Chem.* **2009**, *7*, 598–656. <https://doi.org/10.2478/s11532-009-0097-9>.
4. Švancara, I.; Hvizdalová, M.; Vytřas, K.; Kalcher, K.; Novotný, R. A microscopic study on carbon paste electrodes. *Electroanalysis* **1996**, *8*, 61–65. <https://doi.org/10.1002/elan.1140080113>.
5. Deng, P.-H.; Fei, J.-J.; Feng, Y.-L. Determination of trace vanadium(V) by adsorptive anodic stripping voltammetry on an acetylene black paste electrode in the presence of alizarin violet. *J. Electroanal. Chem.* **2010**, *648*, 85–91. <https://doi.org/10.1016/j.jelechem.2010.08.013>.
6. Liu, Y.; Zhang, L.; Guo, Q.-H.; Hou, H.-Q.; You, T.-Y. Enzyme-free ethanol sensor based on electrospun nickel nanoparticle-loaded carbon fiber paste electrode. *Anal. Chim. Acta* **2010**, *663*, 153–157. <https://doi.org/10.1016/j.aca.2010.01.061>.
7. Hočevar, S.B.; Ogorevc, B. Preparation and characterization of carbon paste micro-electrode based on carbon nanoparticles. *Talanta* **2007**, *74*, 405–411. <https://doi.org/10.1016/j.talanta.2007.10.007>.
8. Miranda Hernandez, A.; Rincon, M.E.; Gonzalez, I. Characterization of carbon-fullerene-silicone oil composite paste electrodes. *Carbon* **2005**, *43*, 1961–1967. <https://doi.org/10.1016/j.carbon.2005.03.004>.
9. Montes, R.; Baeza, M.; Muñoz, J. 0D polymer nanocomposite carbon-paste electrodes using carbon nanohorns: Percolating networks, electrochemical achievements and filler comparison. *Compos. Sci. Technol.* **2020**, *197*, 108260. <https://doi.org/10.1016/j.compscitech.2020.108260>.
10. Rubianes, M.D.; Rivas, G.A. Carbon nanotubes paste electrode. *Electrochem. Commun.* **2003**, *5*, 689–694. [https://doi.org/10.1016/S1388-2481\(03\)00168-1](https://doi.org/10.1016/S1388-2481(03)00168-1).
11. Gasnier, A.; Pedano, M.L.; Rubianes, M.D.; Rivas, G.A. Graphene paste electrode: Electrochemical behavior and analytical applications for the quantification of NADH. *Sens. Actuators B Chem.* **2013**, *176*, 921–926. <https://doi.org/10.1016/j.snb.2012.09.092>.
12. Nantaphol, S.; Channon, R.B.; Kondo, T.; Siangproh, W.; Chailapakul, O.; Henry, C.S. Boron doped diamond paste electrodes for microfluidic paper-based analytical devices. *Anal. Chem.* **2017**, *89*, 4100–4107. <https://doi.org/10.1021/acs.analchem.6b05042>.
13. Skowron, E.; Spilarewicz-Stanek, K.; Guziejewski, D.; Koszelska, K.; Metelka, R.; Smarzewska, S. Analytical performance of clay paste electrode and graphene paste electrode-comparative study. *Molecules* **2022**, *27*, 2037. <https://doi.org/10.3390/molecules27072037>.
14. Torkashvand, M.; Gholivand, M.B.; Taherpour, A.; Boochani, A.; Akhtar, A. Introduction of a carbon paste electrode based on nickel carbide for investigation of interaction between warfarin and vitamin K1. *J. Pharm. Biomed. Anal.* **2017**, *139*, 156–164. <https://doi.org/10.1016/j.jpba.2017.02.032>.
15. Festinger, N.; Morawska, K.; Ivanovski, V.; Ziabka, M.; Jedlińska, K.; Ciesielski, W.; Smarzewska, S. Comparative electroanalytical studies of graphite flake and multilayer graphene paste electrodes. *Sensors* **2020**, *20*, 1684. <https://doi.org/10.3390/s20061684>.

16. Wong, A.; Riojas, A.C.; Baena-Moncada, A.M.; Sotomayor, M.D.P.T. A new electrochemical platform based on carbon black paste electrode modified with  $\alpha$ -cyclodextrin and hierarchical porous carbon used for the simultaneous determination of dipyrone and codeine. *Microchem. J.* **2021**, *164*, 106032. <https://doi.org/10.1016/j.microc.2021.106032>.
17. Liu, L.; Masich, S.; Björk, E.M.; Solin, N.; Inganäs, O. Black charcoal for green and scalable wooden electrodes for supercapacitors. *Energy Technol.* **2022**, *10*, 2101072. <https://doi.org/10.1002/ente.202101072>.
18. Gupta, S.; Mahajan, S.; Gupta, A.; Tathavadkar, V. Method for calcined petroleum coke evaluation to improve the anode quality. In *Light Metals 2023*, 1st ed.; Broek, S., Ed.; Springer Nature Switzerland: Cham, Switzerland, 2023; pp. 1095–1100. [https://doi.org/10.1007/978-3-031-22532-1\\_147](https://doi.org/10.1007/978-3-031-22532-1_147).
19. Altuntas, D.B.; Akgül, G.; Yanik, J.; Anik, Ü. A biochar-modified carbon paste electrode. *Turk. J. Chem.* **2017**, *41*, 455–465. <https://doi.org/10.3906/kim-1610-8>.
20. Gemeiner, P.; Sarakhman, O.; Hatala, M.; Ház, A.; Roupcová, P.; Mackuľak, T.; Barek, J.; Švorc, L. A new generation of fully-printed electrochemical sensors based on biochar/ethylcellulose-modified carbon electrodes: Fabrication, characterization and practical applications. *Electrochim. Acta* **2024**, *487*, 144161. <https://doi.org/10.1016/j.electacta.2024.144161>.
21. Schütter, C.; Ramirez-Castro, C.; Oljaca, M.; Passerini, S.; Winter, M.; Balducci, A. Activated carbon, carbon blacks and graphene based nanoplatelets as active materials for electrochemical double layer capacitors: A comparative study. *J. Electrochem. Soc.* **2015**, *162*, A44–A51. <https://doi.org/10.1149/2.0381501jes>.
22. Balta, Z.; Simsek, E.B. Insights into the photocatalytic behavior of carbon-rich shungite-based WO<sub>3</sub>/TiO<sub>2</sub> catalysts for enhanced dye and pharmaceutical degradation. *New Carbon Mater.* **2020**, *35*, 371–383. [https://doi.org/10.1016/S1872-5805\(20\)60495-4](https://doi.org/10.1016/S1872-5805(20)60495-4).
23. Chou, N.H.; Pierce, N.; Lei, Y.; Perea-López, N.; Fujisawa, K.; Subramanian, S.; Robinson, J.A.; Chen, G.; Omichi, K.; Rozhkov, S.S.; et al. Carbon-rich shungite as a natural resource for efficient Li-ion battery electrodes. *Carbon* **2018**, *130*, 105–111. <https://doi.org/10.1016/j.carbon.2017.12.109>.
24. Bondarenko, S.V.; Tarasevich, Y.I.; Polyakov, V.E.; Zhukova, A.I.; Ivanova, Z.G. Adsorption properties of the natural carbon-mineral sorbent shungite. *Adsorpt. Sci. Technol.* **2008**, *26*, 3–13. <https://doi.org/10.1260/026361708786035413>.
25. Sýs, M.; Bártová, M.; Bartoš, M.; Švancara, I.; Mikysek, T. Shungite (mineralized carbon) as a promising electrode material for electroanalysis. *Materials* **2023**, *16*, 1217. <https://doi.org/10.3390/ma16031217>.
26. Sajo, M.E.J.; Kim, C.-S.; Kim, S.-K.; Shim, K.Y.; Kang, T.-Y.; Lee, K.-J. Antioxidant and anti-inflammatory effects of shungite against ultraviolet B irradiation-induced skin damage in hairless mice. *Oxid. Med. Cell Longev.* **2017**, *2017*, 7340143. <https://doi.org/10.1155/2017/7340143>.
27. Serikbayev, B.; Kamysbayev, D. Electrocatalytic properties of composition systems based on koku shungite. *Bull. Kaz. Nat. Univ.* **2013**, *70*, 91–96. [https://doi.org/https://doi.org/10.15328/chemb\\_2013\\_291-96](https://doi.org/https://doi.org/10.15328/chemb_2013_291-96).
28. Wang, J.; Kirgöz, Ü.A.; Mo, J.-W.; Lu, J.; Kawde, A.N.; Muck, A. Glassy carbon paste electrodes. *Electrochem. Commun.* **2001**, *3*, 203–208. [https://doi.org/10.1016/S1388-2481\(01\)00142-4](https://doi.org/10.1016/S1388-2481(01)00142-4).
29. Królicka, A.; Szczurkowska, A.; Mochalski, P.; Malaita, G. Preparation, characterization, and activation of natural glassy carbon paste electrodes as new sensors for determining the total antioxidant capacity of plant extracts. *Membranes* **2022**, *12*, 1193. <https://doi.org/10.3390/membranes12121193>.
30. Švancara, I.; Vytřas, K.; Metelka, R. Casing for carbon paste for electrochemical measurements. Czech Patent CZ 301714 B6, Int. Cl. G01N 27/30, applied 2nd December 2002, administered 22 April 2010.
31. Figueiredo-Filho, L.C.S.; Brownson, D.A.C.; Gómez-Mingot, M.; Iniesta, J.; Fatibello-Filho, O.; Banks, C.E. Exploring the electrochemical performance of graphitic paste electrodes: Graphene vs. graphite. *Analyst* **2013**, *138*, 6354–6364. <https://doi.org/10.1039/C3AN00950E>.
32. Mikysek, T.; Švancara, I.; Kalcher, K.; Bartoš, M.; Vytřas, K.; Ludvík, J. New approaches to the characterization of carbon paste electrodes using the ohmic resistance effect and qualitative carbon paste indexes. *Anal. Chem.* **2009**, *81*, 6327–6333. <https://doi.org/10.1021/ac9004937>.
33. Sýs, M.; Farag, A.S.; Švancara, I. Extractive stripping voltammetry at carbon paste electrodes for determination of biologically active organic compounds. *Monatsh. Chem.* **2019**, *150*, 373–386. <https://doi.org/10.1007/s00706-018-2346-0>.
34. Borodin, O.; Self, J.; Persson, K.A.; Wang, C.; Xu, K. Uncharted waters: Super-concentrated electrolytes. *Joule* **2020**, *4*, 69–100. <https://doi.org/10.1016/j.joule.2019.12.007>.
35. Morales, D.M.; Risch, M. Seven steps to reliable cyclic voltammetry measurements for the determination of double layer capacitance. *J. Phys. Energy* **2021**, *3*, 034013. <https://doi.org/10.1088/2515-7655/abee33>.
36. Natalia, M.; Sudhakar, Y.N.; Selvakumar, M. Activated carbon derived from natural sources and electrochemical capacitance of double layer capacitance. *Indian J. Chem. Technol.* **2013**, *20*, 392–399.
37. Martínez-Alvarez, O.; Miranda-Hernández, M. Characterization of carbon pastes as matrices in composite electrodes for use in electrochemical capacitors. *Carbon Sci. Tech.* **2008**, *1*, 30–38.
38. Basha, S.I.; Shah, S.S.; Ahmad, S.; Maslehuddin, M.; Al-Zahrani, M.M.; Aziz, M.A. Construction building materials as a potential for structural supercapacitor applications. *Chem. Rec.* **2022**, *22*, e202200134. <https://doi.org/10.1002/tcr.202200134>.
39. Politi, S.; Carcione, R.; Tamburri, E.; Matassa, R.; Lavecchia, T.; Angiellari, M.; Terranova, M.L. Graphene platelets from shungite rock modulate electropolymerization and charge storage mechanisms of soft-template synthesized polypyrrole-based nanocomposites. *Sci. Rep.* **2018**, *8*, 17045. <https://doi.org/10.1038/s41598-018-35415-2>.

40. Fanjul-Bolado, P.; Hernández-Santos, D.; Lamas-Ardisana, P.J.; Martín-Pernía, A.; Costa-García, A. Electrochemical characterization of screen-printed and conventional carbon paste electrodes. *Electrochim. Acta* **2008**, *53*, 3635–3642. <https://doi.org/10.1016/j.electacta.2007.12.044>.
41. Nicholson, R.S. Theory and application of cyclic voltammetry for measurement of electrode reaction kinetics. *Anal. Chem.* **1965**, *37*, 1351–1355. <https://doi.org/10.1021/ac60230a016>.
42. Guidelli, R.; Compton, R.G.; Feliu, J.M.; Gileadi, E.; Lipkowsky, J.; Schmickler, W.; Trasatti, S. Defining the transfer coefficient in electrochemistry: An assessment (IUPAC Technical Report). *Pure Appl. Chem.* **2014**, *86*, 245–258. <https://doi.org/10.1515/pac-2014-5026>.
43. Meléndez, A.M.; Lima, E.; González, I. Influence of the cation Na/Ca/Ag ratio on the ion exchange rate in zeolite A-modified carbon paste electrodes. *J. Phys. Chem. C* **2008**, *112*, 17206–17213. <https://doi.org/10.1021/jp804821c>.
44. Brycht, M.; Łukawska, A.; Frühbauerová, M.; Pravcová, K.; Metelka, R.; Skrzypek, S.; Sýs, M. Rapid monitoring of fungicide fenhexamid residues in selected berries and wine grapes by square-wave voltammetry at carbon-based electrodes. *Food Chem.* **2021**, *338*, 127975. <https://doi.org/10.1016/j.foodchem.2020.127975>.
45. Hart, J.P.; Wring, S.A.; Morgan, I.C. Pre-concentration of vitamin K1(phyloquinone) at carbon paste electrodes and its determination in plasma by adsorptive stripping voltammetry. *Analyst* **1989**, *114*, 933–937. <https://doi.org/10.1039/AN9891400933>.
46. Mehmeti, E.; Stanković, D.M.; Chaiyo, S.; Švorc, L.; Kalcher, K. Manganese dioxide-modified carbon paste electrode for voltammetric determination of riboflavin. *Microchim. Acta* **2016**, *183*, 1619–1624. <https://doi.org/10.1007/s00604-016-1789-4>.
47. Tarasevich, Y.I.; Bondarenko, S.V.; Polyakov, V.E.; Zhukova, A.I.; Ivanova, Z.G.; Luk'yanova, V.V.; Malysh, G.N. The study of the structural, sorption, and electrochemical properties of a natural composite shungite. *Colloid J.* **2008**, *70*, 349–355. <https://doi.org/10.1134/S1061933X08030137>.

**Disclaimer/Publisher's Note:** The statements, opinions and data contained in all publications are solely those of the individual author(s) and contributor(s) and not of MDPI and/or the editor(s). MDPI and/or the editor(s) disclaim responsibility for any injury to people or property resulting from any ideas, methods, instructions or products referred to in the content.